Journal of Statistical Physics, Vol. 90, Nos. 1/2, 1998

Auxiliary Vertices Method for Kagomé-Lattice Eight-Vertex Model

Masafumi Fujimoto[1]

Received April, 1997; final August 12, 1997

We investigate a class of eight-vertex models on a Kagomé lattice. With the help of auxiliary vertices, the Kagomé-lattice eight-vertex model (KEVM) is related to an inhomogeneous system which leads to a one-parameter family of commuting transfer matrices. Using an equation for commuting transfer matrices, we determine their eigenvalues. From calculated eigenvalues the correlation length of the KEVM is derived with its full anisotropy. There are two cases: In the first case the anisotropic correlation length (ACL) is the same as that of the triangular/honeycomb-lattice Ising model. By the use of an algebraic curve, it is shown that the Kagomé-lattice Ising model, the diced-lattice Ising model, and the hard-hexagon model also have (essentially) the same ACL as the KEVM. In the second case we find that the ACL displays 12fold rotational symmetry.

KEY WORDS: Eight-vertex model; auxiliary vertex; anisotropic correlation length; algebraic curve; free state; bound state.

1. INTRODUCTION

Solvable models share a common property that they have commuting transfer matrices.[1-3] The underlying concept is the Yang–Baxter relation. In solving the (square-lattice) eight-vertex model,[4,5] Baxter noticed importance of the relation: As shown in (2.2), the Yang–Baxter relation determines the parametrized forms of the local Boltzmann weights. If the transfer matrix of the eight-vertex model is represented by $\mathbf{V}(u)$, it follows that $\mathbf{V}(u)$ and $\mathbf{V}(u')$ commute with each other for all complex numbers u and u'. The logarithmic derivative of $\mathbf{V}(u)$ at the point $u=-\lambda$ is related to the Hamiltonian $\mathbf{H}$ of the XYZ spin chain.[1,6] For the XYZ spin chain, expanding $\ln \mathbf{V}(u)$ around $u=-\lambda$ gives an infinite number of conserved

[1] Department of Physics, Nara Medical University, Kashihara, Nara 634, Japan.

0022-4715/98/0100-0363$15.00/0

quantities which are involutive. The existence of an infinite number of conserved quantities implies that the Bethe ansatz method[5,7] is applicable to calculations of $\mathbf{H}$ and $\mathbf{V}(u)$. We can find the ground state energy and low-lying excitations of $\mathbf{H}$ and the corresponding eigenvalues of $\mathbf{V}(u)$ by the Bethe ansatz method.

The eight-vertex model can be defined for any four coordinated lattice. By the use of the Yang–Baxter relation, it was shown that a class of eight-vertex models on a Kagomé lattice is solvable.[1,8] (See also refs. 9 and 10.) Baxter[1] obtained the free energy of the Kagomé-lattice eight-vertex model. He also investigated the spontaneous polarization and the horizontal correlation length. Recently, in connection with the equilibrium crystal shape problem,[11] the directional dependence (or anisotropy) of the correlation length and the interfacial tension was calculated for several solvable models.[12–18] For square-lattice models it was pointed out that the equilibrium shape is represented as an algebraic curve. In ref. 18, considering the energy-momentum excitations of a spin chain, we suggested that the algebraic curve is related to a deformation of the pseudo-Euclidian algebra. The Kagomé-lattice eight-vertex model can be regarded as a generalization of the square-lattice eight-vertex model. The situation renders the anisotropic correlation length of the Kagomé-lattice eight-vertex model quite interesting.

In a previous paper[19] we developed a new method to analyze the six-vertex model on a square lattice rotated through an arbitrary angle with respect to the coordinate axes; see also ref. 20. Auxiliary vertices were used to define an inhomogeneous system which still leads to a one-parameter family of commuting transfer matrices. A product of commuting transfer matrices can be interpreted as a transfer matrix acting on zigzag walls in the rotated system. We solved an equation for commuting transfer matrices to determine their eigenvalues. We discussed finite-size properties of the rotated system from the viewpoint of the conformal field theory.

The auxiliary vertices method is widely applicable to analyses of solvable models on triangular, honeycomb, and Kagomé lattices. The application has the advantage that we can utilize various techniques established in calculations of square-lattice models. In this paper we use the auxiliary vertices method to investigate the Kagomé-lattice eight-vertex model defined by Baxter. Our emphases will be on the anisotropy of the correlation length. The present paper is organized as follows: In Section 2 we review some properties of the eight-vertex model. In Section 3, with the help of auxiliary vertices, the Kagomé-lattice eight-vertex model is related to an inhomogeneous system. We consider commuting transfer matrices argument for the inhomogeneous system. In Section 4 we calculate the largest eigenvalues of the commuting transfer matrices. From the results in

Section 4 the anisotropic correlation length is derived in Section 5. Section 6 is devoted to a summary and discussion.

2. SOME PROPERTIES OF MODELS

Suppose a square lattice. The eight-vertex model is represented by drawing an arrow on every edge so that an even number of arrows point into and out of each site (or vertex). We formulate it in terms of arrow-spins. We associate an arrow-spin α_j with each edge j according to the following convention: $\alpha_j = +1$ if the corresponding arrow points up or to the right, and $\alpha_j = -1$ otherwise. Different Boltzmann weights are assigned to the different configurations around a vertex. When arrow-spins around a vertex are ν, α, μ, and β counterclockwise starting from the west edge (Fig. 1), the Boltzmann weight around it is $W(\nu, \alpha \mid \beta, \mu)$ with

$$a = W(++|++) = W(--|--), \quad b = W(+-|-+) = W(-+|+-)$$
$$c = W(+-|+-) = W(-+|-+), \quad d = W(++|--) = W(--|++) \tag{2.1a}$$

and

$$W(\nu, \alpha|\beta, \mu) = 0, \qquad \nu\alpha\beta\mu = -1 \tag{2.1b}$$

The nonzero Boltzmann weights in (2.1) are parametrized as [1]

$$\begin{aligned} a &= -i\rho\Theta(i\lambda)\, H[i(\lambda-u)/2]\, \Theta[i(\lambda+u)/2] \\ b &= -i\rho\Theta(i\lambda)\, \Theta[i(\lambda-u)/2]\, H[i(\lambda+u)/2] \\ c &= -i\rho H(i\lambda)\, \Theta[i(\lambda-u)/2]\, \Theta[i(\lambda+u)/2] \\ d &= i\rho H(i\lambda)\, H[i(\lambda-u)/2]\, H[i(\lambda+u)/2] \end{aligned} \tag{2.2}$$

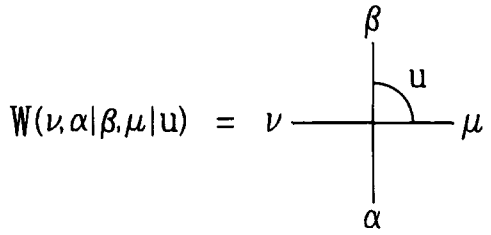

Fig. 1. Boltzmann weight around a vertex.

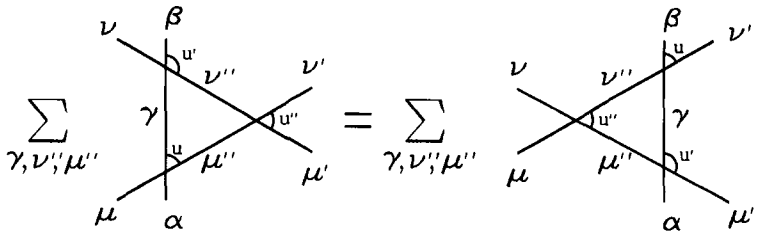

Fig. 2. The Yang–Baxter relation.

where ρ is a normalization factor; the spectral parameter u and the crossing parameter λ appear as arguments of the theta functions. For definitions of the theta functions and related elliptic functions, see Appendix A of ref. 21. We denote the nome by q, the quarter-periods by I and I', and the modulus by k.

We regard λ and k as real constants, and u as a complex variable. The Boltzmann weights W satisfy the Yang–Baxter relation[1-3]

$$\sum_{\gamma,\mu'',\nu''} W(\mu,\alpha|\gamma,\mu''|u)\, W(\nu,\gamma|\beta,\nu''|u')\, W(\nu'',\mu''|\nu',\mu'|u'') = \sum_{\gamma,\mu'',\nu''} W(\nu,\mu|\nu'',\mu''|u)\, W(\mu'',\alpha|\gamma,\mu'|u')\, W(\nu'',\gamma|\beta,\nu'|u) \tag{2.3}$$

for all α, β, μ, ν, μ', $\nu' = \pm 1$ with $u' = u + u'' + \lambda$ (Fig. 2). The Boltzmann weights W also satisfy the following properties:[1-3] the standard initial condition

$$W(\nu,\alpha|\beta,\mu|-\lambda) = -i\rho H(i\lambda)\,\Theta(i\lambda)\,\Theta(0)\,\delta(\nu,\beta)\,\delta(\alpha,\mu) \tag{2.4}$$

the crossing symmetry

$$W(\nu,\alpha|\beta,\mu|-u) = W(\alpha,-\mu|-\nu,\beta|u) \tag{2.5}$$

and the local inversion relation

$$\sum_{\alpha',\beta'} W(\alpha,\beta|\alpha',\beta'|-u-2\lambda)\, W(\alpha',\beta'|\alpha'',\beta''|u) = -\rho^2 h[(u+3\lambda)/2]\, h[(u-\lambda)/2]\,\delta(\alpha,\alpha'')\,\delta(\beta,\beta'') \tag{2.6}$$

where $\delta(\cdot,\cdot)$ denotes the Kronecker symbol and $h(u)$ is defined by

$$h(u) = -i\Theta(0)\,\Theta(iu)\,H(iu) \tag{2.7}$$

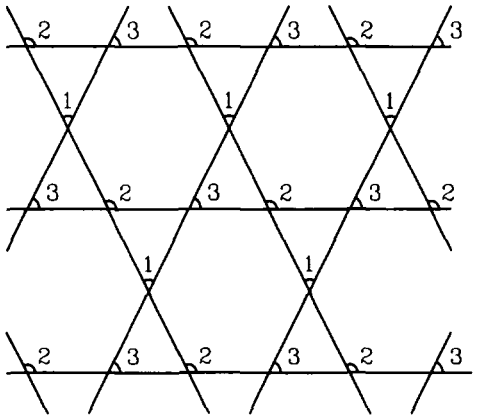

Fig. 3. Kagomé-lattice eight-vertex model.

From (2.4) and (2.5) it follows that

$$W(v, \alpha \mid \beta, \mu \mid \lambda) = -ip H(i\lambda)\, \Theta(i\lambda)\, \Theta(0)\, \delta(v, -\alpha)\, \delta(\beta, -\mu) \qquad (2.4')$$

Using (2.3), Baxter showed that a class of eight-vertex models on a Kagomé lattice is solvable.[1] In a Kagomé lattice[22] there are three types of vertices; let us call them 1, 2, and 3 (Fig. 3). Assume that all vertices of the same type have the same Boltzmann weights. We denote by a_1 the

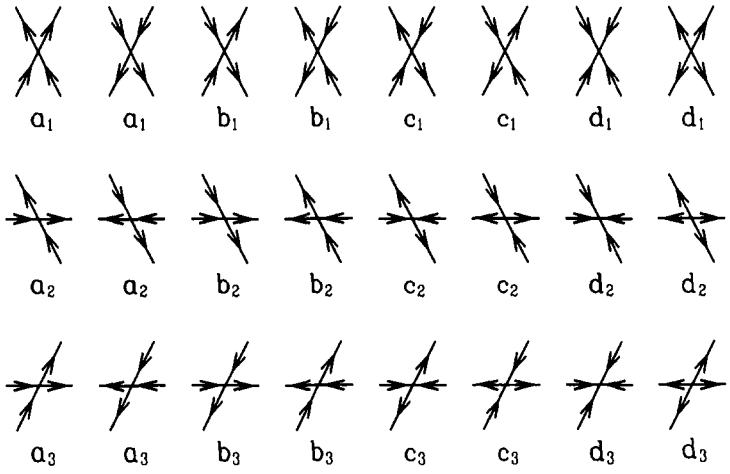

Fig. 4. Three types of vertices on the Kagomé lattice. The corrsponding Boltzmann weights are shown underneath.

value of a for vertices of type 1; and b_1, c_1, d_1, a_2, b_2, c_2, d_2, a_3, b_3, c_3, d_3 are introduced similarly. For a vertex of type j we order arrow configurations around it as in the jth row of Fig. 4. We consider the case that the Boltzmann weights a_1, b_1, c_1, d_1 are given by (2.2), and those of types 2 and 3 by (2.2) with the spectral parameter u replaced by $u'(=u+u''+\lambda)$ and u'', respectively. In this case the Yang–Baxter relation (2.3) implies that we can shift horizontal lines without changing the partition function; see Figs. 11.5 and 11.6 of ref. 1. The Kagomé lattice can be deformed into a lattice consisting of three square-lattice regions: in the upper (or lower) region there exists an inhomogeneous eight-vertex model; in the central region the square lattice is drawn diagonally. Baxter used the deformation to calculate the free energy of the Kagomé-lattice eight-vertex model. Moreover, Baxter found that the correlation length along the horizontal direction is the same as that of the square-lattice eight-vertex model along the diagonal direction.

3. AUXILIARY VERTICES METHODS

We explain a method to investigate the Kagomé-lattice eight-vertex model. We start by defining an inhomogeneous system.[19–20] Suppose a square lattice of $2M$ columns and $4N$ rows with periodic boundary conditions in both directions. We also assume that the spectral parameter u can vary from site to site. The value of u for the site (i, j) are denoted by u_{ij}. Set the u_{ij} to be

$$u_{ij}=\begin{cases} v'' & \text{for } i\equiv 0 \pmod 2,\quad j\equiv 0,2 \pmod 4 \\ v' & \text{for } i\equiv 1 \pmod 2,\quad j\equiv 0,2 \pmod 4 \\ -\lambda & \text{for } i\equiv 0 \pmod 2,\quad j\equiv 1 \pmod 4 \\ v & \text{for } i\equiv 1 \pmod 2,\quad j\equiv 1 \pmod 4 \\ -v & \text{for } i\equiv 0 \pmod 2,\quad j\equiv 3 \pmod 4 \\ \lambda & \text{for } i\equiv 1 \pmod 2,\quad j\equiv 3 \pmod 4 \end{cases} \tag{3.1}$$

with

$$v'=v+v''+\lambda \tag{3.2}$$

(Fig. 5a), and the normalization factor ρ to be

$$\rho=i/H(i\lambda)\,\Theta(i\lambda)\,\Theta(0) \tag{3.3}$$

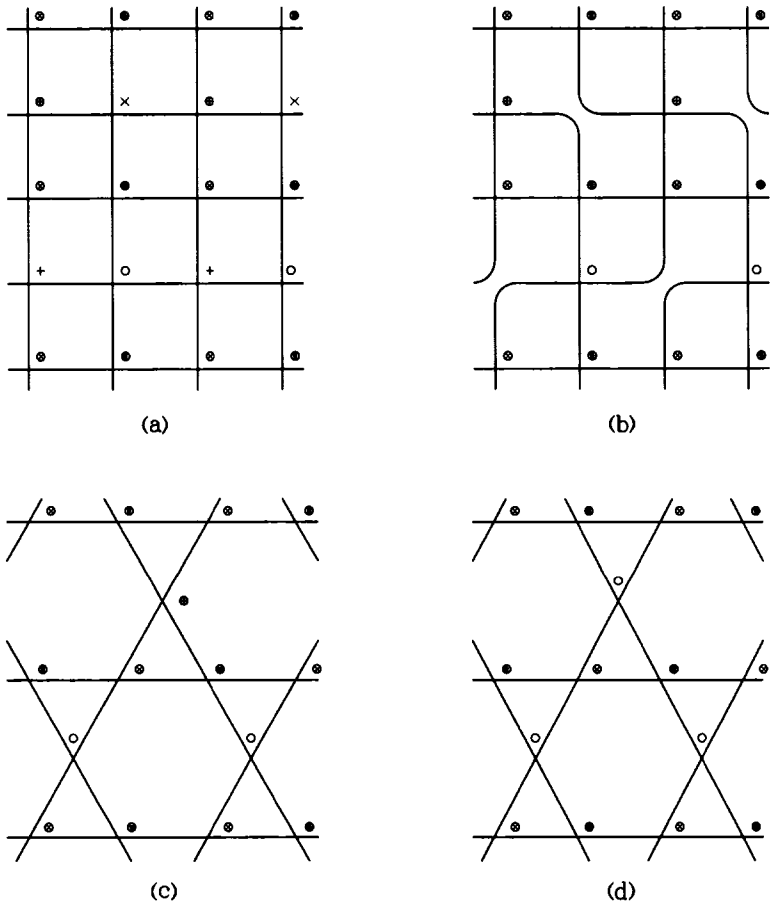

Fig. 5. (a) Inhomogeneous system (3.1). Vertices $u = v$ (respectively v', v'', $-v$, λ, $-\lambda$) are presented by ○ (respectively ⊙, ⊗, ⊕, ×, +). (b) Decomposing auxiliary vertices $u = \lambda$ and $-\lambda$, we deform the square lattice into a Kagomé lattice. (c) The Kagomé lattice consists of four kinds of vertices: $u = \pm v$, v', and v''. (d) Using the crossing symmetry, we find that the inhomogeneous system (3.1) is equivalent to the Kagomé-lattice eight-vertex model.

In this paper analyses are restricted to an antiferroelectric ordered regime

$$0 < k < 1, \qquad 0 < \lambda < I', \qquad -\lambda < v < -v'' < \lambda \tag{3.4}$$

The inhomogeneous system is related to the eight-vertex model on a Kagomé lattice. To see this, we decompose auxiliary vertices.[19] In (3.1)

vertices $u_{ij} = \pm\lambda$ are auxiliary ones. We separate the east and south edges from the west and north ones at each auxiliary vertex $u_{ij} = -\lambda$. The separation yields two types of corners. Because of the standard initial condition (2.4), there is one arrow pointing in and one arrow pointing out at each corner. We can regard two edges meeting at a corner as a bonding where an arrow is placed. Auxiliary vertices $u_{ij} = \lambda$ are decomposed in a similar way: instead of (2.4), (2.4′) is used to separate the east and north edges from the west and south ones. After all the auxiliary vertices are decomposed (Fig. 5b), we can continuously deform the square lattice into a Kagomé lattice. The Kagomé lattice consists of four types of vertices: $u_{ij} = \pm v$, v', and v'' (Fig. 5c). Note that the orientation of vertices $u_{ij} = v$ is different from that of $u_{ij} = -v$. We use the crossing symmetry (2.5) to change the orientation of vertices $u_{ij} = -v$, with their spectral parameter $-v$ replaced by v. It follows that the inhomogeneous system (3.1) is equivalent to the Kagomé-lattice eight-vertex model defined by Baxter (Fig. 5d). Thus, we can analyze the Kagomé-lattice eight-vertex model by considering the inhomogeneous system (3.1).

The inhomogeneous system (3.1) is investigated by commuting transfer matrices argument.[1] Let $\bar{\alpha} = \{\alpha_0, \alpha_1, ..., \alpha_{2M-1}\}$ and $\bar{\beta} = \{\beta_0, \beta_1, ..., \beta_{2M-1}\}$ be the arrow-spins on two successive rows of vertical edges, and $\bar{\mu} = \{\mu_0, \mu_1, ..., \mu_{2M-1}\}$ the arrow-spins on a row intervening between $\bar{\alpha}$ and $\bar{\beta}$. We define inhomogeneous transfer matrices by

$$[\mathbf{V}_{\mathrm{IH}}(u)]_{\bar{\alpha},\bar{\beta}} = \sum_{\bar{\mu}} \prod_{j=0}^{M-1} W(\mu_{2j}, \alpha_{2j} | \beta_{2j}, \mu_{2j+1} | u) \times W(\mu_{2j+1}, \alpha_{2j+1} | \beta_{2j+1}, \mu_{2j+2} | u + \lambda + v) \tag{3.5}$$

where $\mu_{2M} = \mu_0$. From the Yang–Baxter relation (2.3), we find that the inhomogeneous transfer matrices form a one-parameter family of commuting transfer matrices.

We can construct a nonsingular matrix $\mathbf{Q}(u)$ which satisfies the matrix equation[1, 5, 16]

$$\mathbf{V}_{\mathrm{IH}}(u)\,\mathbf{Q}(u) = \phi(u-\lambda)\,\mathbf{Q}(u+2\lambda') + \phi(u+\lambda)\,\mathbf{Q}(u-2\lambda') \tag{3.6}$$

where $\lambda' = \lambda - 2iI$ and

$$\phi(u) = \rho^{2M}\{h[u/2]\,h[(u+v+\lambda)/2]\}^M \tag{3.7}$$

with $h(u)$ defined by (2.7). Since $\mathbf{Q}(u)$ commutes with $\mathbf{Q}(u')$ and $\mathbf{V}_{\mathrm{IH}}(u'')$ for all complex numbers u, u', and u'', the matrix equation (3.6) gives the eigenvalue equation

$$\begin{aligned} V_{\mathrm{IH}}(u)\, Q(u) &= \phi(u-\lambda)\, Q(u+2\lambda') + \phi(u+\lambda)\, Q(u-2\lambda') \\ &= \phi(u+\lambda)\, Q(u-2\lambda')[1+P(u)] \end{aligned} \tag{3.8}$$

with

$$P(u) = \phi(u-\lambda)\, Q(u+2\lambda')/\phi(u+\lambda)\, Q(u-2\lambda') \tag{3.9}$$

where we denote the eigenvalues of $\mathbf{V}_{\mathrm{IH}}(u)$ by $V_{\mathrm{IH}}(u)$, and the corresponding ones of $\mathbf{Q}(u)$ by $Q(u)$.

Two matrices $\mathbf{O}$ and $\mathbf{R}$ are introduced; $\mathbf{O}$ is a diagonal matrix with entries $+1$ (respectively -1) for arrow configurations of an even (respectively odd) number of down arrows; $\mathbf{R}$ has the effect of reversing all arrows. The matrices $\mathbf{O}$, $\mathbf{R}$, $\mathbf{Q}(u)$, and $\mathbf{V}_{\mathrm{IH}}(u')$ commute with each other for all complex numbers u and u'. The eigenvalues of $\mathbf{O}$ (respectively $\mathbf{R}$) are denoted by O (respectively R); note that R take a value of $+1$ or -1. Detailed analyses show that $Q(u)$ must be of the form

$$Q(u) = \exp(tu) \prod_{j=1}^{M} h[(u-u_j)/2] \tag{3.10}$$

The zeros u_j and a constant t are determined by the condition that the rhs of (3.8) vanishes

$$\begin{aligned} &\left\{\frac{h[(u_j-\lambda)/2]}{h[(u_j+\lambda)/2]}\frac{h[(u_j+v)/2]}{h[(u_j+2\lambda+v)/2]}\right\}^{M} \\ &\quad = -\exp(-4t\lambda') \times \prod_{k=1}^{M} \frac{h[(u_j-u_k-2\lambda)/2]}{h[(u_j-u_k+2\lambda)/2]}, \qquad j=1, 2,..., M \end{aligned} \tag{3.11}$$

and the sum rules

$$\begin{aligned} &u_1+u_2+\cdots+u_M+(\lambda+v)M/2 \\ &\quad = (O-1+2M)\, I'/2 + i(OR-1+2M)\, I + 2p'I' + 4piI \end{aligned} \tag{3.12a}$$

$$t = (O-1+2M+4p')\, \pi/8I \tag{3.12b}$$

where p and p' are integers. Solving (3.11) with (3.12), and then using (3.10) in (3.8) with solutions u_j and t, we can determine the eigenvalues

$V_{\mathrm{IH}}(u)$. There are many eigenvalues corresponding to different solutions of (3.11).

After the eigenvalues $V_{\mathrm{IH}}(u)$ are calculated, we can get necessary information to investigate the inhomogeneous system (3.1) and hence the Kagomé-lattice eight-vertex model by letting $u=-v$, $-\lambda$, and v''. The partition function of the Kagomé-lattice eight-vertex model is calculated as

$$Z=\mathrm{Tr}[\mathbf{T}^N]=\sum_j T_j^N \tag{3.13}$$

with

$$\mathbf{T}=\mathbf{V}_{\mathrm{IH}}(v'')\,\mathbf{V}_{\mathrm{IH}}(-\lambda)\,\mathbf{V}_{\mathrm{IH}}(v'')\,\mathbf{V}_{\mathrm{IH}}(-v) \tag{3.14a}$$

$$T_j=V_{\mathrm{IH};j}(v'')\,V_{\mathrm{IH};j}(-\lambda)\,V_{\mathrm{IH};j}(v'')\,V_{\mathrm{IH};j}(-v) \tag{3.14b}$$

where $\mathbf{T}$ corresponds to the transfer matrix of the Kagomé-lattice eight-vertex model and T_j [or $V_{\mathrm{IH};j}(u)$] is the jth eigenvalue of $\mathbf{T}$ [or $\mathbf{V}_{\mathrm{IH}}(u)$] in decreasing order of magnitude.

The anisotropic correlation length of the Kagomé-lattice eight-vertex model can be found by considering the correlation length between two vertical arrows α_{00} and $\alpha_{2m,4n}$ in the inhomogeneous system (3.1). We introduce an operator $\mathbf{S}$ by

$$\mathbf{S}=g(v)\,\mathbf{V}_{\mathrm{IH}}(-\lambda)\,\mathbf{V}_{\mathrm{IH}}(-v-2\lambda) \tag{3.15}$$

with

$$g(u)=\{-\rho^2 h[(u+3\lambda)/2]\,h[(u-\lambda)/2]\}^{-M} \tag{3.16}$$

Because of the local inversion relation (2.6), $\mathbf{S}$ has the effect of shifting an arrow configuration on a row of vertical edges by two lattice spacings: $\{\alpha_0, \alpha_1, \alpha_2,\ldots, \alpha_{2M-1}\} \to \{\alpha_{2M-2}, \alpha_{2M-1}, \alpha_0,\ldots, \alpha_{2M-3}\}$. The expectation value $\langle \alpha_{00}\alpha_{2m,4n}\rangle$ is represented as[15]

$$\langle \alpha_{00}\alpha_{2m,4n}\rangle = Z^{-1}\mathrm{Tr}[\mathbf{A}\mathbf{T}^n\mathbf{S}^{-m}\mathbf{A}\mathbf{S}^m\mathbf{T}^{N-n}] \tag{3.17}$$

with a diagonal matrix $\mathbf{A}$ defined by

$$[\mathbf{A}]_{\alpha,\bar{\beta}}=\begin{cases}\alpha_0 & \text{if } \alpha=\bar{\beta}\\ 0 & \text{otherwise}\end{cases} \tag{3.18}$$

Applying a similarity transformation which diagonalizes $\mathbf{V}(u)$, and taking the $N, M \to \infty$ limit, we obtain

$$\langle \alpha_{00} \alpha_{2m,4n} \rangle = \sum_j [\tilde{\mathbf{A}}]_{0,j} [\tilde{\mathbf{A}}]_{j,0} \left[\frac{T_j}{T_0} \left(\frac{S_j}{S_0} \right)^{\eta} \right]^n \tag{3.19}$$

where $\eta = -m/n$, $\tilde{\mathbf{A}}$ is the matrix transformed from $\mathbf{A}$, and S_j is the jth eigenvalue of $\mathbf{S}$:

$$S_j = g(v)\, V_{\mathrm{IH};j}(-\lambda)\, V_{\mathrm{IH};j}(-v-2\lambda) \tag{3.20}$$

Eq. (3.19) shows that we can find the correlation length of the Kagomé-lattice eight-vertex model along the direction designated by η from the ratios of the eigenvalues of the transfer matrix $\mathbf{T}$ and the corresponding ones of the shift operator $\mathbf{S}$.

4. LARGEST EIGENVALUES

In this section we solve (3.7)–(3.12) to find the eigenvalues $V_{\mathrm{IH}}(u)$. These kinds of calculations are usually achieved by introducing a distribution function of the zeros u_j.[23] This approach is a very cumbersome one, however. We use another approach.[1, 16, 21, 24–25] Methods are somewhat indirect. Instead of the distribution of u_j, analytic properties of the functions in (3.8) are investigated. Using the analytic properties, we determine asymptotic forms of $V_{\mathrm{IH}}(u)$ as $M \to \infty$.

Note that in the regime (3.4) two antiferroelectric ordered states are degenerate. It is expected that there exists a doublet of largest eigenvalues in $-\lambda < \mathrm{Re}(u) < -v$. To calculate these eigenvalues, we repeat almost the same argument in Section 3 of ref. 16; see also refs. 1 and 24. As a beginning, we investigate the zero-temperature limit. The zero-temperature limit corresponds to the $k \to 0$ and $I', \lambda, v, u \to \infty$ limit with the ratios λ/I', v/I', u/I' being order of unity. We find a doublet of eigenvalues labeled by $O = O_0 = (-)^M$ and $R = \pm 1$; the two eigenvalues are denoted by $V_{\mathrm{IH};\pm}(u)$. For $V_{\mathrm{IH};R}(u)$ the zeros u_j are given by

$$u_j \sim (2I/M)\, i[2j - M - (R+1)/2] - (\lambda + v)/2, \qquad j = 1, 2, \ldots, M \tag{4.1}$$

In a vertical strip which contains the line $\mathrm{Re}(u) = -(\lambda + v)/2$, the function $P(u)$ is estimated as

$$P_R(u) \sim R(-)^M x^{M/2} y^{M/2} z^M \tag{4.2}$$

where

$$x = \exp(-\pi\lambda/2I), \qquad y = \exp(-\pi v/2I), \qquad z = \exp(-\pi u/2I) \tag{4.3}$$

When M becomes large, the asymptotic form of $V_{\mathrm{IH};R}(u)$ is

$$\begin{aligned} V_{\mathrm{IH};R}(u) &\sim R\rho^{2M} q^{M/2} x^{-2M} (1 - qz/x)^M (1 - q/x^2 yz)^M \\ &\sim R c^M(u)\, c^M(u + v + \lambda), \qquad -2\lambda - v < \mathrm{Re}(u) < \lambda \end{aligned} \tag{4.4}$$

From (4.4) we identify the two eigenvalues $V_{\mathrm{IH};R}(u)$ as the doublet of largest eigenvalues. The corresponding eigenstates are called ground states.

Here, we turn to nonzero temperatures. The zero-temperature results (4.1)–(4.4) suggest that

(i) for large M the zeros u_j lie on the line $\mathrm{Re}(u) = -(\lambda + v)/2$,

(ii) there exists a real positive number δ such that $P_R(u)$ is exponentially larger than 1 as $M \to \infty$ for $-\delta < \mathrm{Re}(u) + (\lambda + v)/2 < 0$; $P_R(u)$ is exponentially smaller than 1 for $0 < \mathrm{Re}(u) + (\lambda + v)/2 < \delta$,

(iii) $V_{\mathrm{IH};R}(u)$ is analytic and nonzero in a vertical strip containing the line $\mathrm{Re}(u) = -(\lambda + v)/2$.

Assuming the properties (i)–(iii), and after some calculations, we obtain

$$\begin{aligned} P_R(u) &\sim R p^M(u)\, p^M(u + \lambda + v), && |\mathrm{Re}(u) + (\lambda + v)/2| < \min\{2\lambda, 2I' - 2\lambda\} \\ &\sim 1, && 2\lambda < \mathrm{Re}(u) + (\lambda + v)/2 < 2I' - 2\lambda \\ &\sim p^M(u)\, p^M(u - 2I')\, p^M(u + \lambda + v)\, p^M(u + \lambda + v - 2I'), \\ & && 2I' - 2\lambda < \mathrm{Re}(u) + (\lambda + v)/2 < 2\lambda \end{aligned} \tag{4.5}$$

with

$$\begin{aligned} p(u) &= (-z)^{1/2} f(xz^{-1}, x^4)/f(xz, x^4) \\ f(a, b) &= (1 - a) \prod_{n=1}^{\infty} (1 - ab^n)(1 - a^{-1}b^n)(1 - b^n) \end{aligned} \tag{4.6}$$

(See Appendix B of ref. 16.)

The asymptotic form of the doublet of largest eigenvalues as $M \to \infty$ are determined as

$$V_{\mathrm{IH};R}(u) \sim R\kappa(u)\, \kappa(u + \lambda + v), \qquad -\lambda < \mathrm{Re}(u) < -v \tag{4.7}$$

where

$$\kappa(u)=\left(\frac{\gamma\rho}{x}\right)^{M}\prod_{n=0}^{\infty}\frac{A[u+(4n+3)\lambda]\,A[u+2I'+(4n-1)\lambda]}{A[u+(4n+5)\lambda]\,A[u+2I'+(4n+1)\lambda]}$$
$$\times\frac{A[(4n+3)\lambda-u]\,A[(4n-1)\lambda-u+2I']}{A[(4n+5)\lambda-u]\,A[(4n+1)\lambda-u+2I']} \tag{4.8}$$

with

$$\gamma=q^{1/4}\Theta(0)\prod_{n=1}^{\infty}(1-q^{2n})^2,\qquad A(u)=\prod_{n=0}^{\infty}(1-q^n z)^M \tag{4.9}$$

Eqs. (4.5) and (4.7) are consistent with the three conditions (i)–(iii). In the $k\to 0$ limit (4.5) reproduces (4.2) along the line $\mathrm{Re}(u)=-(\lambda+v)/2$, and (4.7) reproduces (4.4) for $-\lambda<\mathrm{Re}(u)<-v$. These facts verify the correctness of the argument. The zero-temperature result (4.4) implies that (4.7) is analytically continued into $-2\lambda-v<\mathrm{Re}(u)<\lambda$.

In (4.7) the two eigenvalues $V_{\mathrm{IH};R}(u)$ are equal in magnitude and opposite in sign. This degeneracy cannot occur for finite M by the Perron–Frobenius theorem. Calculations of finite-size correction terms show that $V_{\mathrm{IH};R}(u)$ are asymptotically degenerate as $M\to\infty$:[1, 16, 24]

$$-V_{\mathrm{IH};+}(u)/V_{\mathrm{IH};-}(u)$$
$$\sim 1+\alpha(u)\,p^M[2iI+(\lambda-v)/2]\,p^M[2iI+(3\lambda+v)/2] \tag{4.10}$$
$$-\lambda<\mathrm{Re}(u)<-v$$

(Note that the finite-size correction term on the rhs is positive and exponentially smaller than 1.)

In addition to the doublet of largest eigenvalues, we can derive the asymptotic forms of the next-largest eigenvalues, the neat-next-largest eigenvalues, and so on. For these eigenvalues it is expected that $\mathrm{Re}(u_j)\neq -(\lambda+v)/2$ for a finite number of zeros and the other zeros are continuously distributed on the line $\mathrm{Re}(u)=-(\lambda+v)/2$. We have to distinguish between the two subregimes $0<\lambda<I'/2$ and $I'/2<\lambda<I'$: in the subregime $0<\lambda<I'/2$ all the excitations are superpositions of so-called free states, whereas in the subregime $I'/2<\lambda<I'$ there exist bound states besides the free states.[23]

Firstly, we consider the subregime $0<\lambda<I'/2$. We use a method developed in ref. 21. Eq. (4.5) shows that, when M becomes large, $P_+(u)$ behaves as

$$P_+(u)=\begin{cases} O(e^M), & -2\lambda<\mathrm{Re}(u)+(\lambda+v)/2<0 \\ O(e^{-M}), & 0<\mathrm{Re}(u)+(\lambda+v)/2<2\lambda \\ 1, & 2\lambda<\mathrm{Re}(u)+(\lambda+v)/2<2I'-2\lambda \end{cases} \tag{4.11}$$

We find that $P(u)$ has the same exponential behavior with possible exception of some isolated points. It follows that for large M

$$V_{\mathrm{IH}}(u)/V_{\mathrm{IH};+}(u)\sim(O/O_0) \times\begin{cases} Q(u+2\lambda)Q_+(u)/Q_+(u+2\lambda)Q(u), & -2\lambda<\mathrm{Re}(u)+(\lambda+v)/2<0 \\ Q(u-2\lambda)Q_+(u)/Q_+(u-2\lambda)Q(u), & 0<\mathrm{Re}(u)+(\lambda+v)/2<2\lambda \end{cases} \tag{4.12}$$

Limiting functions are introduced by

$$L(u)=\lim_{M\to\infty} V_{\mathrm{IH}}(u)/V_{\mathrm{IH};+}(u) \tag{4.13a}$$

$$G(u)=\lim_{M\to\infty} Q(u)/Q_+(u) \tag{4.13b}$$

where we denote the eigenvalue $Q(u)$ corresponding to $V_{\mathrm{IH};+}(u)$ by $Q_+(u)$. Taking the $M\to\infty$ limit in (4.12) gives

$$L(u)=(O/O_0) \times\begin{cases} G(u+2\lambda)/G(u), & -2\lambda<\mathrm{Re}(u)+(\lambda+v)/2<0 \\ G(u-2\lambda)/G(u), & 0<\mathrm{Re}(u)+(\lambda+v)/2<2\lambda \end{cases} \tag{4.14}$$

We obtain the inversion relation

$$L(u)\,L(u+2\lambda)=1, \qquad -2\lambda<\mathrm{Re}(u)+(\lambda+v)/2<0 \tag{4.15}$$

We can prove that $V_{\mathrm{IH}}(u)/V_{\mathrm{IH};+}(u)$ converges as $M\to\infty$ in a vertical strip containing the line $\mathrm{Re}(u)=-(\lambda+v)/2$, and that the limiting function $L(u)$ is analytic there; see Appendix E of ref. 21.

The limiting function $L(u)$ can be continued so that the inversion relation (4.15) is valid everywhere in the complex plane. The continued function $L(u)$ is meromorphic and doubly periodic:

$$L(u+4iI)=L(u+4\lambda)=L(u) \tag{4.16}$$

It follows that $L(u)$ must be of the form

$$L(u) = \pm \prod_{\text{zeros}} p(u - u_z + \lambda) \prod_{\text{poles}} p(u - u_p - \lambda)$$
$$-2\lambda < \mathrm{Re}(u) + (\lambda + v)/2 < 2\lambda \tag{4.17}$$

where u_z and u_p represent zeros and poles of $L(u)$ in the rectangle $[-2\lambda, 0) \times [-2iI, -2iI)$, respectively. The zeros for which $\mathrm{Re}(u_j) \neq -(\lambda + v)/2$ are grouped pairwise with distance 2λ in $|\mathrm{Re}(u) + (\lambda + v)/2| < 2\lambda$. Those occur as singles in $2\lambda < \mathrm{Re}(u) + (\lambda + v)/2 < 2I' - 2\lambda$. For both cases it is shown that $L(u)$ is analytic and nonzero in $0 < |\mathrm{Re}(u) + (\lambda + v)/2| < 2\lambda$. We obtain

$$L(u) = \pm \prod_{j=1}^{v} p[u - \Theta_j + (3\lambda + v)/2], \quad -2\lambda < \mathrm{Re}(u) + (\lambda + v)/2 < 2\lambda \tag{4.18}$$

with an even integer v and imaginary free parameters Θ_j $(j = 1, 2, \ldots, v)$, which is just a superposition of free states. For the next-largest eigenvalues there are superpositions with $O = \pm O_0$ and $R = \pm 1$; the limiting function is

$$L_1(u) = \pm p[u - \Theta_1 + (3\lambda + v)/2]\, p[u - \Theta_2 + (3\lambda + v)/2]$$
$$-2\lambda < \mathrm{Re}(u) + (\lambda + v)/2 < 2\lambda \tag{4.19}$$

Secondly, we investigate the subregime $I'/2 < \lambda < I'$. In this subregime bound states appear besides free states. Repeating almost the same argument, we can prove that (4.17) is satisfied in a region including the vertical strip $-2\lambda - v < \mathrm{Re}(u) < \lambda$. It is found that the zeros which do not lie on the line $\mathrm{Re}(u_j) = -(\lambda + v)/2$ form strings with $(2I' - 2\lambda)$-spacing and endpoints u_L, u_R in $0 < \mathrm{Re}(u) + (\lambda + v)/2 < I'$, $I' < \mathrm{Re}(u) + (\lambda + v)/2 < 2I'$, respectively. The strings are classified into two types. In a type I string μ-zeros are distributed symmetrically about the line $\mathrm{Re}(u) = -(\lambda + v)/2 + I'$, where $1 \leqslant \mu \leqslant [I'/(I' - \lambda)] - 1$ and $[a]$ is the largest integer $\leqslant a$. A type II string consists of $\mu = [I'/(I' - \lambda)]$ or $[I'/(I' - \lambda)] + 1$ zeros, whose distribution is not necessarily symmetric about the line $\mathrm{Re}(u) = -(\lambda + v)/2 + I'$. (See Appendix C of ref. 25.) The contribution from a type I string to the product in (4.17) is given by

$$p[u - \Theta + d_\mu + (3\lambda + v)/2]\, p[u - \Theta - d_\mu + (3\lambda + v)/2] \tag{4.20}$$

where Θ is an imaginary free parameter and

$$d_\mu = (\mu + 1)\,\lambda - \mu I' \tag{4.21}$$

The corresponding excitation is a bound state of two free particles. The contribution from a type II string to the product in (4.17) is

$$p[u - \Theta_1 + (3\lambda + v)/2]\; p[u - \Theta_2 + (3\lambda + v)/2] \tag{4.22}$$

with imaginary free parameters Θ_1 and Θ_2.

In the subregime $I'/2 < \lambda < I'$ the lowest excitations are dominated by bound states with $\mu = 1$, $O = -O_0$, and $R = \pm 1$. The limiting function for the next-largest eigenvalues is

$$L_1(u) = \pm p[u - \Theta + d_1 + (3\lambda + v)/2]\; p[u - \Theta - d_1 + (3\lambda + v)/2] \tag{4.23}$$

Situations for higher excitations are somewhat complicated. We have to divide the subregime into some regions. For example, to consider the next-next-largest eigenvalues, the subregime is divided into two regions: Eq. (4.22), which comes from free states with $O = \pm O_0$ and $R = \pm 1$, gives the expression for the next-next-largest eigenvalues in the region $I'/2 < \lambda < 2I'/3$; the next-next-largest eigenvalues corresponds to bound states with $\mu = 2$, $O = O_0$, and $R = \pm 1$ in the region $2I'/3 < \lambda < I'$; thus, we obtain for the next-next-largest eigenvalues

$$L_2(u) = \begin{cases} \pm p[u - \Theta_1 + (3\lambda + v)/2]\; p[u - \Theta_2 + (3\lambda + v)/2], & I'/2 < \lambda < 2I'/3 \\ \pm p[u - \Theta + d_2 + (3\lambda + v)/2]\; p[u - \Theta - d_2 + (3\lambda + v)/2], & 2I'/3 < \lambda < I' \end{cases} \tag{4.24}$$

5. ANISOTROPIC CORRELATION LENGTH

Now, using the results in Section 4, we calculate the anisotropic correlation length ξ of the Kagomé-lattice eight-vertex model. Firstly we consider the subregime $0 < \lambda < I'/2$, and then the subregime $I'/2 < \lambda < I'$.

As shown in Section 3, the Kagomé-lattice eight-vertex model is equivalent to the inhomogeneous system (3.1). Using the expression (3.19), we consider the anisotropic correlation length in the subregime $0 < \lambda < I'/2$. From (3.14b), (3.20), and (4.13a), it follows that

$$\lim_{M\to\infty} T/T_+ = L(v'')^2\, L(-v)\, L(-\lambda) \tag{5.1a}$$

$$\lim_{M\to\infty} S/S_+ = L(-\lambda)\, L(-v-2\lambda) \tag{5.1b}$$

We note that the matrix elements $[\tilde{\mathbf{A}}]_{0,j}$ and $[\tilde{\mathbf{A}}]_{j,0}$ in (3.19) vanish if $O=-O_0$ or $R=+1$ for the jth eigenvalue.[17,23] When n becomes large with $\eta=-m/n$ fixed, only the band of next-largest eigenvalues with $O=O_0$ and $R=-1$ contribute to the leading asymptotic behavior of the correlation function. Use (5.1) with (4.19) in (3.19). The summation in (3.19) becomes an integral over the imaginary parameters Θ_1 and Θ_2 because of a continuous distribution of the next-largest eigenvalues. We obtain

$$\begin{aligned}\langle \alpha_{00}\alpha_{2m4n}\rangle - \langle \alpha_{00}\rangle\langle \alpha_{2m4n}\rangle \sim \int_{-4iI}^{4iI} d\Theta_1 \int_{-4iI}^{4iI} d\Theta_2\, \rho(\Theta_1,\Theta_2)\\ \{p^2[v''-\Theta_1+(3\lambda+v)/2]\; p^2[-\Theta_1+(\lambda+v)/2]\\ \times\{p[-\Theta_1+(\lambda+v)/2]\; p[-\Theta_1-(\lambda+v)/2]\}^{-1+\eta}\}^n\\ \times(\textit{the same factors with } \Theta_1\to\Theta_2)\end{aligned} \tag{5.2}$$

where the function $\rho(\Theta_1,\Theta_2)$ is to be determined from the distribution of the eigenvalues and the matrix elements $[\tilde{\mathbf{A}}]_{0,j}$, $[\tilde{\mathbf{A}}]_{j,0}$; its explicit form is not important here.

We regard triangles in the Kagomé-lattice eight-vertex model as equilateral ones with unit edge lengths (Fig. 5d). We denote by θ the angle between the vertical axis and the direction along which the correlation length is calculated. The ratio η is connected with θ by

$$\eta=\sqrt{3}\tan\theta \tag{5.3}$$

Estimating the integral on the rhs of (5.2) by the method of steepest descent, we find the correlation length ξ of the Kagomé-lattice eight-vertex model:

$$\begin{aligned}1/\xi = -\frac{2}{\sqrt{3}}\cos\theta \ln|p[v''-\Theta_s+(3\lambda+v)/2]\; p[-\Theta_s+(\lambda+v)/2]|\\ -\frac{2}{\sqrt{3}}\sin\left(\theta-\frac{\pi}{6}\right)\ln|p[-\Theta_s+(\lambda+v)/2]\; p[-\Theta_s-(\lambda+v)/2]|\end{aligned} \tag{5.4}$$

where Θ_s is a saddle point determined as a function of θ by

$$\cos\theta \frac{p[-2\Theta_s+\lambda+v+v'']}{p[v''-\Theta_s+(3\lambda+v)/2]\,p[-\Theta_s+(\lambda+v)/2]} \times\{1-p^2[v''-\Theta_s+(3\lambda+v)/2]\,p^2[-\Theta_s+(\lambda+v)/2]\} + \sin\left(\theta-\frac{\pi}{6}\right)\frac{p[-2\Theta_s-\lambda]}{p[-\Theta_s+(\lambda+v)/2]\,p[-\Theta_s-(\lambda+v)/2]} \times\{1-p^2[-\Theta_s+(\lambda+v)/2]\,p^2[-\Theta_s-(\lambda+v)/2]\}=0 \quad (5.5)$$

with

$$\Theta_s=-\lambda+2iI, \qquad \theta=\pi/2 \quad (5.6)$$

Fig. 6a is the polar plot of $1/\xi$ given by (5.4)–(5.6) with $v=v''=-\lambda/3$, where interactions of the model are isotropic.

In the subregime $I'/2<\lambda<I'$ the next-largest eigenvalues cannot contribute to the asymptotic behavior of the correlation function since they correspond to $O=-O_0$ and $R=\pm 1$. The asymptotic behavior of the correlation function is determined by the next-next-largest eigenvalues with $O=O_0$ and $R=-1$. We use (4.24) instead of (4.19). Note that the first equation of (4.24) is identical with (4.19). For $I'/2<\lambda<2I'/3$ the anisotropic correlation length is the same as that of the subregime $0<\lambda<I'/2$. For $2I'/3<\lambda<I'$, substituting (5.1) with the second equation of (4.24) into (3.19), we find that

$$\langle\alpha_{00}\alpha_{2m4n}\rangle-\langle\alpha_{00}\rangle\langle\alpha_{2m4n}\rangle\sim\int_{-4iI}^{4iI}d\Theta\rho(\Theta) \{p^2[v''-\Theta+d_2+(3\lambda+v)/2]\,p^2[-\Theta+d_2+(\lambda+v)/2] \times\{p[-\Theta+d_2+(\lambda+v)/2]\,p[-\Theta+d_2-(\lambda+v)/2]\}^{-1+\eta}\}^n \times(\textit{the same factors with } d_2\to -d_2) \quad (5.7)$$

where the summation in (3.19) becomes the integral along the imaginary axis and the function $\rho(\Theta)$ is to be determined from the distribution of the eigenvalues and the matrix elements $[\tilde{\mathbf{A}}]_{0,j}$, $[\tilde{\mathbf{A}}]_{j,0}$. Integrate it by the method of steepest descent. It follows that

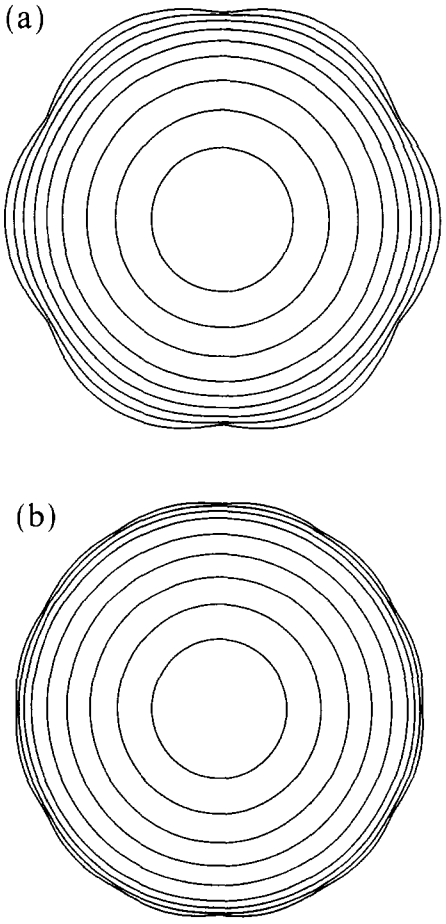

Fig. 6. (a) The polar plot of $1/\xi$ for $0<\lambda<2I'/3$ and $v=v''=-\lambda/3$. From the outermost figure, $x=1\times10^{-6}$, 0.0001, 0.001, 0.004, 0.01, 0.02, 0.04, 0.07, 0.12, successively. (b) The polar plot of $1/\xi$ with $\lambda=12I'/17$ and $v=v''=-\lambda/3$. From the outermost figure, $x=1\times10^{-10}$, 1×10^{-6}, 0.00001, 0.0001, 0.001, 0.004, 0.016, 0.05, 0.12. (Each figure is suitably scaled.)

$$
\begin{aligned}
1/\xi = &-\frac{1}{\sqrt{3}}\cos\theta\{\ln|p[v''-\Theta_s+d_2+(3\lambda+v)/2]\,p[-\Theta_s+d_2+(\lambda+v)/2]|\}\\
&-\frac{1}{\sqrt{3}}\sin\left(\theta-\frac{\pi}{6}\right)\{\ln|p[-\Theta_s+d_2+(\lambda+v)/2]\\
&\times p[-\Theta_s+d_2-(\lambda+v)/2]|\}\\
&+(\textit{the same terms with } d_2\to-d_2)
\end{aligned}
\tag{5.8}
$$

where the saddle point Θ_s is determined as a function of θ by

$$\cos\theta\left\{\frac{p[-2\Theta_s+2d_2+\lambda+v+v'']}{p[v''-\Theta_s+d_2+(3\lambda+v)/2]\,p[-\Theta_s+d_2+(\lambda+v)/2]}\right.$$
$$\left.\times\{1-p^2[v''-\Theta_s+d_2+(3\lambda+v)/2]\,p^2[-\Theta_s+d_2+(\lambda+v)/2]\}\right\}$$
$$+\sin\left(\theta-\frac{\pi}{6}\right)\left\{\frac{p[-2\Theta_s+2d_2-\lambda]}{p[-\Theta_s+d_2+(\lambda+v)/2]\,p[-\Theta_s+d_2-(\lambda+v)/2]}\right.$$
$$\left.\times\{1-p^2[-\Theta_s+d_2+(\lambda+v)/2]\,p^2[-\Theta_s+d_2-(\lambda+v)/2]\}\right\}$$
$$+(\textit{the same terms with } d_2\to -d_2)=0 \tag{5.9}$$

with (5.6). The polar plot of $1/\xi$ given by (5.6), (5.8)–(5.9) with $v=v''=-\lambda/3$ and $I'=17\lambda/12$ is shown in Fig. 6b.

6. SUMMARY AND DISCUSSION

In this paper we investigated a class of eight-vertex models on a Kagomé lattice, a model defined by Baxter. Analyses were restricted to the antiferroelectric ordered regime

$$0<q<x^2<1, \qquad x<y''^{-1}<y<x^{-1} \tag{6.1}$$

where q is the nome of the theta functions in (2.2), x and y are defined by (4.3), and

$$y''=\exp(-\pi v''/2I) \tag{6.2}$$

Auxiliary vertices were introduced into the model to relate it to an inhomogeneous system which possesses a one-parameter family of commuting transfer matrices. The transfer matrix and the shift operator of the Kagomé-lattice eight-vertex model were represented as products of commuting transfer matrices. Using an equation, we determined the eigenvalues of the commuting family. From the calculated eigenvalues the correlation length ξ of the Kagomé-lattice eight-vertex model was derived with its full anisotropy.

There were two cases with respect to the parameter q: $0<q<x^3$ and $x^3<q<x^2$. In the case $0<q<x^3$ the anisotropic correlation length is independent of q. Baxter showed that the Kagomé-lattice eight-vertex model

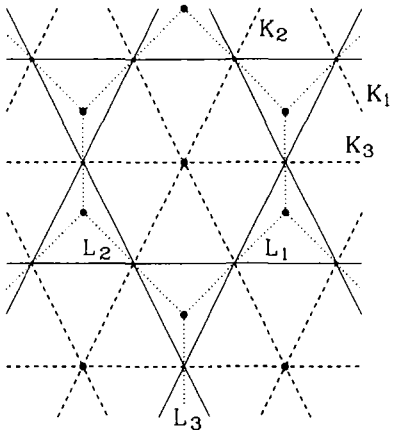

Fig. 7. In the $q \to x^4$ limit the Kagomé-lattice eight-vertex model is decoupled into two Ising models; one is on a triangular lattice, and the other on a honeycomb lattice. The (eight-vertex model) Kagomé lattice is shown by solid lines, the (Ising model) triangular lattice by broken lines, and the (Ising model) honey-comb lattice by dotted lines.

can be regarded as an Ising model with two- and four-spin interactions.[1] In the $q \to x^4$ limit the Ising model is decoupled into two nearest-neighbor Ising models; one is on a triangular lattice, and the other on a honeycomb lattice (Fig. 7). The two nearest-neighbor Ising models are connected with each other by the star-triangle relation. The interaction coefficients of the triangular-lattice Ising model are given by

$$\begin{aligned} \sinh 2K_1 &= 1/k_1 \operatorname{snh}[I_1(\lambda - v'')/2I] \\ \sinh 2K_2 &= 1/k_1 \operatorname{snh}[I_1(\lambda + v')/2I] \\ \sinh 2K_3 &= 1/k_1 \operatorname{snh}[I_1(\lambda - v)/2I] \end{aligned} \tag{6.3}$$

where the snh function is defined by (*A*.2) of ref. 21 with the quarter-periods I_1 and I_1' which satisfy $I_1'/I_1 = \lambda/I$. The interaction coefficients L_1, L_2, and L_3 of the honeycomb-lattice Ising model are related to those of the triangular-lattice Ising model by

$$\sinh 2K_j \sinh 2L_j = k_1^{-1}, \qquad j = 1, 2, 3 \tag{6.4}$$

It is noted that the triangular-lattice Ising model and the honeycomb-lattice Ising model have the same anisotropic correlation length; see, for example, ref. 12. In the decoupling limit $q \to x^4$ we find that for all directions

$$\xi = 2\xi_{\text{t/h}} \tag{6.5}$$

where $\xi_{t/h}$ is the anisotropic correlation length of the triangular/honeycomb-lattice Ising model; the factor 2 is because of a change of lattice spacing.

It is helpful to consider the Wulff construction[11]

$$\Lambda X/k_B T = (1/\xi)\cos\theta - \frac{d(1/\xi)}{d\theta}\sin\theta \tag{6.6a}$$

$$\Lambda Y/k_B T = (1/\xi)\sin\theta + \frac{d(1/\xi)}{d\theta}\cos\theta \tag{6.6b}$$

where Λ is a scale factor. Substituting (5.4) into (6.6), we obtain

$$\begin{aligned}\alpha &= \exp[-\Lambda(\sqrt{3}\,X/2 - Y/2)/k_B T] \\ &= p[v'' - \Theta_s + (3\lambda + v)/2]/p[-\Theta_s - (\lambda + v)/2]\end{aligned} \tag{6.7a}$$

$$\begin{aligned}\beta &= \exp[-\Lambda Y/k_B T] \\ &= p[-\Theta_s + (\lambda + v)/2]\; p[-\Theta_s - (\lambda + v)/2]\end{aligned} \tag{6.7b}$$

The Wulff construction (6.6) gives a one-to-one correspondence between the anisotropic correlation length ξ and the shape (6.7). We can rewrite (6.7) into a compact form

$$(\alpha\beta + \alpha^{-1}\beta^{-1}) + A(\alpha + \alpha^{-1}) + B(\beta + \beta^{-1}) = C \tag{6.8}$$

with

$$A = \mathrm{snh}[I_1(\lambda - v'')/2I]/\mathrm{snh}[I_1(\lambda + v')/2I] \tag{6.9a}$$

$$B = \mathrm{snh}[I_1(\lambda - v'')/2I]/\mathrm{snh}[I_1(\lambda - v)/2I] \tag{6.9b}$$

$$\begin{aligned}C = 2\{&\mathrm{dnh}[I_1(\lambda - v'')/2I]\;\mathrm{dnh}[I_1(\lambda + v')/2I]\;\mathrm{dnh}[I_1(\lambda - v)/2I] + 1\} \\ &/k_1^2\,\mathrm{snh}[I_1(\lambda + v')/2I]\;\mathrm{snh}[I_1(\lambda - v)/2I]\end{aligned} \tag{6.9c}$$

For any Ising model on a planar lattice, it was shown that the interfacial tension is related to the correlation length on a dual lattice above the critical temperature.[13] Using the relation and the Wulff construction, Holtzer[14] derived the equilibrium crystal shapes of various planar Ising models. See Table I of ref. 14, and compare the shape (6.8) with the equilibrium crystal shapes of the Kagomé-lattice Ising model and the diced-lattice Ising model. We find that the anisotropic correlation length in the case $0 < q < x^3$ is the same as those of the two Ising models (above the critical temperature). In ref. 15 the anisotropic correlation length of the hard-hexagon model was calculated. We note that the function $\phi(a)$ defined by

(2.13b) of ref. 15 is equivalent to the product $p[-\Theta+\lambda/3]\ p[-\Theta-\lambda/3]$. It follows that the anisotropic correlation length of the hard-hexagon model in the disordered phase is written into the form (6.8) with $v=v''=-\lambda/3$ and λ replaced by $\lambda+3Ii$. Thus, the anisotropic correlation length in the case $0<q<x^3$ and that of the hard-hexagon model in the disordered phase are of the same type. We expect that a wide class of models have (essentially) the same anisotropic correlation length as the Kagomé-lattice eight-vertex model has in the case $0<q<x^3$. Furthermore, in (5.1b) and (5.2), (S/S_+) was expressed by the use of $L_1(u)$ in (4.19) or $L_2(u)$ given by the first equation of (4.24). We can regard the expression as a product of a limiting function which corresponds to bound states of two free particles; compare it with (4.20), for example. It is found that (6.8) corresponds to a special limit of the algebraic curve (4.6) in ref. 17; see also ref. 18.

In (4.10) we showed that the doublet of largest eigenvalues $V_{\mathrm{IH};\pm}(u)$ are asymptotically degenerate as $M\to\infty$. The interfacial tension σ of the Kagomé-lattice eight-vertex model along the horizontal direction $\theta=\pi/2$ is derived from the finite-size correction terms there.[1, 15-16, 24] It follows that

$$2\sigma/k_{\mathrm{B}}T=1/\xi \qquad \text{for} \quad \theta=\pi/2 \tag{6.10}$$

The auxiliary vertices method is easily generalized to calculate the anisotropic interfacial tension of the Kagomé-lattice eight-vertex model. We can prove that (6.10) is satisfied for all directions. Detailed calculations about this point will be reported in next publication.

In the case $x^3<q<x^2$ the anisotropic correlation length ξ depends on the parameter q. In (5.1b) and (5.7) we represented (S/S_+) by the use of $L_2(u)$ given by the second equation of (4.24). This expression can be regarded as a limiting function corresponding to bound states of four free particles. It is expected that the anisotropic correlation length in the case $x^3<q<x^2$ is also a general one. We note that the anisotropic correlation length ξ possesses twelvefold rotational symmetry in a special limit of this case. Recently, Widom [26] showed that the Bethe ansatz method is applicable to tilings of the plane by squares and equilateral triangles. The random tiling model displays twelvefold rotational symmetry. Analysis of the anisotropic correlation length of the random tiling model is desirable. We hope that this problem will be solved in further investigations.

We can obtain the anisotropic correlation length of the Kagomé-lattice eight-vertex model in other regimes from the analysis in the antiferroelectric ordered regime (6.1). At last, we calculate the anisotropic correlation length ξ^* in a disordered regime. We represent the Boltzmann weights for the three types of vertices in the disordered regime as a_j^*, b_j^*, c_j^*, and d_j^*

($j=1, 2, 3$). The Boltzmann weights a_j^*, b_j^*, c_j^*, d_j^* in the disordered regime are related to those of the regime (6.1) by

$$\begin{aligned} a_j^* &= (a_j - b_j + c_j - d_j)/2, \qquad b_j^* = (-a_j + b_j + c_j - d_j)/2 \\ c_j^* &= (a_j + b_j + c_j + d_j)/2, \qquad d_j^* = (-a_j - b_j + c_j + d_j)/2 \end{aligned} \tag{6.11}$$

for $j=1, 2, 3$. In stead of (3.19), we start with (2.13) and (2.17) of ref. 23. In (2.17) of ref. 23, the eigenvalues Λ_j are replaced by T_j. Moreover, we introduce the eigenvalues S_j of the shift operator into the expression.

For $0<q<x^4$ we use (5.1) with the limiting function (4.19); the anisotropic correlation length ξ^* is derived from an integral over the band of next-largest eigenvalues corresponding to free states with $O=-O_0$ and $R=-1$. It follows that

$$\xi^* = \xi \tag{6.12}$$

for all directions. In the decoupling limit $q \to x^4$ we obtain

$$\xi^* = \xi_{\mathrm{t/h}}^* \tag{6.13}$$

where $\xi_{\mathrm{t/h}}^*$ is the anisotropic correlation length of the triangular/honeycomb-lattice Ising model above the critical temperature; the interaction coefficients K_j^* and L_j^* of the Ising model above the critical temperature is related to K_j and L_j by

$$\mathrm{e}^{-2K_j^*} = \tanh L_j, \quad \mathrm{e}^{-2L_j^*} = \tanh K_j, \qquad j=1, 2, 3 \tag{6.14}$$

We find that for all directions

$$\xi_{\mathrm{t/h}} = \xi_{\mathrm{t/h}}^*/2 \tag{6.15}$$

The anisotropic interfacial tension $\sigma_{\mathrm{t/h}}$ of the triangular/honeycomb-lattice Ising model is connected with the anisotropic interfacial tension σ of the Kagomé-lattice eight-vertex model by

$$2\sigma = \sigma_{\mathrm{t/h}} \tag{6.16}$$

Eqs. (6.10), (6.12), (6.13), and (6.16) imply that

$$1/\xi_{\mathrm{t/h}}^* = \sigma_{\mathrm{t/h}}/k_{\mathrm{B}}T \tag{6.17}$$

(See ref. 12.)

For $x^4<q<x^2$ the anisotropic correlation length ξ^* in the disordered regime is determined by the band of next-largest eigenvalues corresponding

to bound states with $O = -O_0$ and $R = -1$. Substitute (4.23) into (5.1). After some calculations, we find that ξ^* is given by

$$\begin{aligned} 1/\xi^* = &-\frac{1}{\sqrt{3}}\cos\theta\{\ln|p[v''-\Theta_s+d_1+(3\lambda+v)/2] \\ &\times p[-\Theta_s+d_1+(\lambda+v)/2]|\} \\ &-\frac{1}{\sqrt{3}}\sin\left(\theta-\frac{\pi}{6}\right)\{\ln|p[-\Theta_s+d_1+(\lambda+v)/2] \\ &\times p[-\Theta_s+d_1-(\lambda+v)/2]|\} \\ &+(\textit{the same terms with } d_1 \to -d_1) \end{aligned} \tag{6.18}$$

with the saddle point Θ_s determined by

$$\begin{aligned} \cos\theta &\left\{\frac{p[-2\Theta_s+2d_1+\lambda+v+v'']}{p[v''-\Theta_s+d_1+(3\lambda+v)/2]\,p[-\Theta_s+d_1+(\lambda+v)/2]}\right. \\ &\left.\times\{1-p^2[v''-\Theta_s+d_1+(3\lambda+v)/2]\,p^2[-\Theta_s+d_1+(\lambda+v)/2]\}\right\} \\ &+\sin\left(\theta-\frac{\pi}{6}\right)\left\{\frac{p[-2\Theta_s+2d_1-\lambda]}{p[-\Theta_s+d_1+(\lambda+v)/2]\,p[-\Theta_s+d_1-(\lambda+v)/2]}\right. \\ &\left.\times\{1-p^2[-\Theta_s+d_1+(\lambda+v)/2]\,p^2[-\Theta_s+d_1-(\lambda+v)/2]\}\right\} \\ &+(\textit{the same terms with } d_1 \to -d_1)=0 \end{aligned} \tag{6.19}$$

and

$$\Theta_s = -\lambda + 2iI, \qquad \theta = \pi/2 \tag{6.20}$$

where d_1 is defined by (4.21).

REFERENCES

1. R. J. Baxter, *Exactly Solved Models in Statistical Mechanics* (Academic Press, London, 1982).
2. M. Wadati and Y. Akutsu, *Prog. Theor. Phys. Suppl.* **94**:1–41 (1988).
3. M. Wadati, T. Deguchi, and Y. Akutsu, *Phys. Rep.* **180**:247–332 (1989).
4. R. J. Baxter, *Phys. Rev. Lett.* **26**:832–833 (1971); *Ann. Phys. (N. Y.)* **70**:193–228 (1972).
5. R. J. Baxter, *Ann. Phys. (N. Y.)* **76**:1–24, 25–47, 48–71 (1973).
6. R. J. Baxter, *Phys. Rev. Lett.* **26**:834 (1971); *Ann. Phys. (N. Y.)* **70**:323–337 (1972).

7. H. A. Bethe, *Z. Phys.* **71**:205–226 (1931).
8. T. T. Truong and K. D. Schotte, *Nucl. Phys. B* **220[FS8]**:77–101 (1983).
9. R. J. Baxter and I. G. Enting, *J. Phys. A:Math. Gen.* **11**:2463–2473 (1978).
10. R. J. Baxter, H. N. V. Temperley, and S. E. Ashley, *Proc. R. Soc. Lond. A* **358**:535–559 (1978).
11. G. Wulff, *Z. Krist. Mineral.* **34**:449–530 (1901); C. Herring, *Phys. Rev.* **82**:87–93 (1951); W. K. Burton, N. Cabrela, and F. C. Frank, *Phil. R. Soc. A* **243**:229–358 (1951).
12. R. K. P. Zia, *J. Stat. Phys.* **45**:801–813 (1986).
13. M. Holtzer, *Phys. Rev. Lett.* **64**:653–656 (1990); Y. Akutsu and N. Akutsu, *Phys. Rev. Lett.* **64**:1189–1192 (1990).
14. M. Holtzer, *Phys. Rev. B* **42**:10570–10582 (1990).
15. M. Fujimoto, *J. Stat. Phys.* **59**:1355–1381 (1990).
16. M. Fujimoto, *J. Stat. Phys.* **67**:123–154 (1992).
17. M. Fujimoto, *Physica A* **233**:485–502 (1996).
18. M. Fujimoto, *J. Phys. A:Math. Gen.* **30**:3779–3793 (1997).
19. M. Fujimoto, *J. Stat. Phys.* **82**:1519–1539 (1996).
20. M. Fujimoto, *J. Phys. A:Math. Gen.* **27**:5101–5119 (1994).
21. A. Klümper and J. Zittartz, *Z. Phys. B* **71**:495–507 (1988).
22. I. Syozi, *Prog. Theor. Phys.* **6**:306–308 (1951).
23. J. D. Johnson, S. Krinsky, and B. M. McCoy, *Phys. Rev. A* **8**:2526–2547 (1973).
24. R. J. Baxter, *J. Stat. Phys.* **8**:25–55 (1973).
25. A. Klümper and J. Zittartz, *Z. Phys. B* **75**:371–384 (1989).
26. M. Widom, *Phys. Rev. Lett.* **70**:2094–2097 (1993).